Nanoscale

Accepted Manuscript

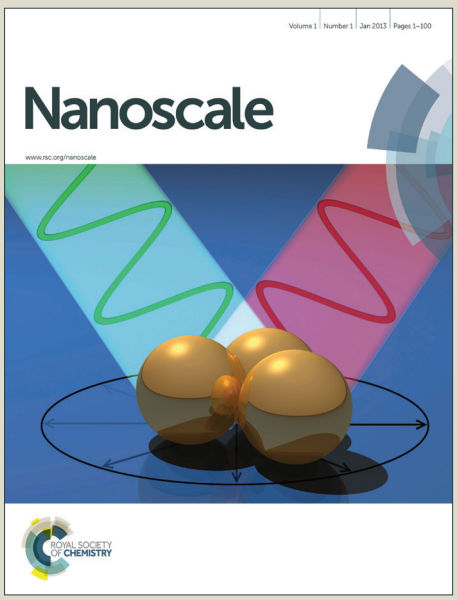

ROYAL SOCIETY OF CHEMISTRY

www.rsc.org/nanoscale

Cite this: DOI: 10.1039/c0xx00000x

www.rsc.org/xxxxxx

ARTICLE TYPE

Facile and eco-friendly synthesis of green fluorescent carbon nanodots for bioimaging, patterning and staining

Lihong Shi[a,*], Yanyan Li[a], Xiaofeng Li[b], Xiangping Wen[a], Guomei Zhang[a], Jun Yang[a], Chuan Dong[a], Shaomin Shuang[a]

Received (in XXX, XXX) Xth XXXXXXXXX 20XX, Accepted Xth XXXXXXXXX 20XX
DOI: 10.1039/b000000x

We report a facile and eco-friendly strategy for fabrication of green fluorescent carbon nanodots (CDs), and demonstrate their applications for bio-imaging, patterning, and staining. One-pot hydrothermal method of various plant petals yields bright green-emitting CDs, providing an easy way for the production of green fluorescent CDs without the request of tedious synthetic methodology or the use of toxic/expensive solvents and starting materials. The as-prepared CDs show small size distribution and excellent dispersibility. Their strong green fluorescence is observed when the excitation wavelength is between 430 nm and 490 nm. Moreover, they exhibit high tolerance to various external conditions, such as pH values, external cations, and continuous excitation. Due to minimum toxicity as well as good photoluminescent properties, these CDs can be applied to in vitro and in vivo imaging, patterning, and staining. According to confocal fluorescent imaging of human uterine cervical squamous cell carcinoma cells, CDs penetrate into the cell and enter cytoplasm and nucleus. More strikingly, carp is directly fed with CDs for in vivo imaging and shows bright green fluorescence at an excitation wavelength of 470 nm. Additionally, the obtained CDs are used as fluorescent inks for drawing luminescent patterns. Finally, we also apply the CDs as fluorescent dye. Interestingly, absorbent filter paper with staining emits dramatic fluorescence under 470 nm excitation.

1. Introduction

Fluorescent nanoparticles have a tremendous impact on the advancement of a wide range of fields including electronics, photonics, energy, catalysis, and medicine. To date, typical photoluminescent (PL) particles have been developed from compounds of lead, cadmium, gold, silver, and silicon. But these materials also have raised concerns over potential toxicity, environmental harm and high cost.[1] Therefore, it is very desirable to develop a simple and eco-friendly method for the synthesis of fluorescent nanoparticles with good photostability and low toxicity.

Fluorescent carbon nanodots (CDs), a young smart member of the carbon nanomaterial family, were first obtained during purification of single-walled carbon nanotubes in 2004.[2] They are generally defined as carbon nanomaterials with sizes below 10 nm and considered to consist of an amorphous or crystalline core with predominant sp^2 carbon and an oxidized carbon shell with carboxyl group. By virtue of their low cost, high aqueous solubility, low photobleaching, non-blinking, low toxicity, and excellent biocompatibility, fluorescent CDs have great promise for a variety of practical applications, such as bioimaging,[1] chemical sensor and biosensor,[3−5] drug delivery,[6] gene delivery,[7] dye sensitizers,[8] catalysis,[9,10] fluorescent ink,[11] and mimetics peroxidase.[12]

Currently, CDs are typically synthesized by two types of strategies: top-down and bottom-up routes. Top-down approaches involve laser ablation or electrochemical oxidation of graphite,[13,14] electrochemical treatment of multiwalled carbon nanotubes,[15] and chemical oxidation of commercially activated carbon.[16] Bottom-up methods include pyrolysis,[17,18] wet oxidation,[19,20] hydrothermal synthesis,[21−24] and microwave-assisted synthesis.[11,25] Undoubtly, the preparation of CDs should be simple and environmentally benign as far as possible. Among preparation methods of CDs, the hydrothermal synthesis is a rising technique, due to simple experimental setup, easy control of the reaction, and low energy consumption.[26,27] Additionally, a green method using precursors directly from nature is highly desired and would be of great benefit to large scale synthesis and widespread applications.

By far, most of CDs emit blue luminescence under UV irradiation. In the case of bio-imaging, CDs with blue luminescence might be less favorable as optical nanoprobes due to the autofluorescence. The green luminescent CDs appear to be an attractive alternative. Moreover, such green luminescent CDs offer unique opportunities to gain complementary insights in the relationship between the physiochemical and optical properties. However, limited CDs with green fluorescence have been reported. Sun et al[28] developed green PL CDs by laser ablation and subsequent doping with ZnO or ZnS. Liu et al[29] described a synthetic approach for green fluorescent graphene quantum dots from ethylene glycol in the presence of concentrated sulfuric acid.

Wang et al[30] reported green fluorescent CDs by microwave of phytic acid and ethylene diamine. Liu et al[31] applied an effective approach to prepare green luminescent CDs by one-step microwave method, in which sugars role as carbon source and diethylene glycol role as reaction medium. Li et al[32] mixed sugars and bases to get green luminescent CDs. Nevertheless, all these methods suffer from some drawbacks like the requirement of tedious synthetic methodology or the use of toxic/expensive solvents and starting materials. Thus the production of CDs from renewable bio-precursors with easy and inexpensive methods is a challenging but worthy concept.

In the present work, green fluorescent CDs are prepared from plant petals by one-step hydrothermal treatment for the first time. The process is environmentally friendly, simple, and efficient. Coupled with low toxicity and good PL properties, the as-synthesized CDs have been successfully utilized to bio-imaging, patterning, and staining.

2. Experimental

2.1. Materials

$AlCl_3$, $BaCl_2$, $CaCl_2$, $CdCl_2$, $CoCl_2$, $CuCl_2$, $FeCl_3$, $FeCl_2$, $HgCl_2$, KCl, $MgCl_2$, $MnCl_2$, NaCl, $NiCl_2$, and $ZnCl_2$ were purchased from Beijing Chemical Corp. (Beijing, China). NaH_2PO_4 and Na_2HPO_4 were purchased from Shanghai Aladdin Reagent Co., Ltd. (Shanghai, China). The petals including lily petal, Chinese rose petals, Sophora japonica petals, Rosa yellow petals, Hollyhock petals and Petunia petals, which were picked from the campus of Shanxi University and Azalea petals, Erythrina corallodendron petals and Magnolia petals, which were picked from the campus of Chongqing University of Posts and Telecommunications, and were washed with water and then dried in air prior to use. Rhodamin 6G was obtained from E.Merck, Darmstadt. 3-(4,5-dimethylthiazol-2-yl)-2,5-diphenyltetrazolium bromide (MTT) was obtained from Solarbio (Beijing, China). Distilled deionized (DDI) water was obtained from a Millipore Milli-Q-RO4 water purification system with a resistivity 18.2 $M\Omega \cdot cm^{-1}$ (Bedford, MA, USA). All the reagents were used as received without further purication. Deionized water was used in experiments.

2.2. Synthesis of CDs

CDs were prepared by hydrothermal treatment of petals. Typically, the petals were first grounded into powder. Petals (0.5 g) was dissolved in deionized water (20 mL) at room temperature. The cloudy solution was poured into a 50 mL high pressure reactor vessel, then placed in an oven, and heated under the conditions of 250°C for 3 h. After cooling down to room temperature, the CDs were collected by removing larger particles through centrifugation at 5000 rpm for 20 min. The as-prepared CDs derived from Aralia petals, Hollyhock petals, Morning Glory petals, Lily petals, Chinese Rose petals, Sophora japonica petals, Azalea petals, Magnolia petals, and the yellow Rosa petals are referred to as CD_{Ara}, CD_{Hol}, CD_{Mor}, CD_{Lil}, CD_{Ros}, CD_{SJ}, CD_{Aza}, CD_{Mag}, and CD_{Yel}, respectively.

Additionally, we chose Aralia petals, Hollyhock petals, and Morning Glory petals to fabricate CDs at different reaction temperature and reaction time.

2.3. Fluorescence QY measurements

The relative fluorescence QY (Φ) of the CDs was calculated using the equation of $\Phi_x = \Phi_{std} I_x A_{std} \eta^2_x / (I_{std} A_x \eta^2_{std})$. The optical densities were measured on Puxi TU-1901 UV-vis absorption spectrophotometer. In the equation, I_x and I_{std} are the fluorescence intensities of the CDs and the standard, and A_x and A_{std} are the optical densities (OD) of the CDs and the standard, respectively. Rhodamin 6G in ethanol was chosen as a standard with a quantum yield $\Phi_{std} = 0.94$ at 488 nm. η_x and η_{std} are the refractive index of the CDs and the standard, respectively. The absorbencies of all the samples in 1.0 cm cuvette were kept under 0.1 at the excitation wavelength to minimize re-absorption effects.

2.4. Characterization

Transmission electron microscopy (TEM) study was carried out in a JEOL JEM-2100 instrument operating at an accelerating voltage of 200 kV. Samples for TEM measurements were prepared by placing a drop of colloidal solution on carbon-coated copper grid and then dried at room temperature. The size distribution of CDs was performed by counting over 132 particles. Fluorescent photographs of CDs under 470 nm excitation were operated with a multispectral fluorescent vivo molecular imaging system (S-0010A). Fourier Transform infrared (FTIR) spectra were recorded on Bruker tensor 2 spectrometer using a resolution of 4 cm^{-1}. The sample with 1 mg diluted by KBr (ratio 1:200) was pressed into the disc. X-ray photoelectron spectroscopy (XPS) data were obtained with an AXIS ULTRA DLD electron spectrometer from Shimadzu company using 300 W Al Kα radiation. The base pressure was about 3×10^{-9} mbar and the binding energies were referenced to the C_{1s} line at 284.6 eV from adventitious carbon. UV-visible absorption spectra of CDs were recorded by HITACHI U-2910 UV. Fluorescence spectra were operated with Hitachi F-4500 fluorescence spectrophotometer. Fluorescence lifetime were measured by the Edinburgh FLS920.

2.5 MTT assay

For the cell cytotoxicity text, human uterine cervical squamous cell carcinoma (A193) cells were first plated on a Costar 96-well tissue-culture cluster and cultured at 37°C with 5% CO_2 in air for 3 h to adhere cells onto the surface. The well without cells and treatment with CD_{Ara} was taken as a zero set. The medium was then changed with 100 μL of fresh DMEM supplemented with 10% FBS containing CD_{Ara}, and the cells were allowed to grow for another 24 h. At least five parallel samples were performed in each group. Cells without treatment with CD_{Ara} were taken as a control. After adding 20 μL of 5.0 mg/mL MTT reagent into every well, the cells were further incubated for 4 h, followed by removing the culture medium with MTT, and then 150 μL of DMSO was added. The resulting mixture was shaken for *ca.* 10 min at room temperature. The *OD* of the mixture was measured at 490 nm with a SunRisemicroplate reader (Tecan Austria GmbH, Grödig, Austria). The cell viability was estimated using the equation of *Cell Viability* (%) = $(OD_{Treated}/OD_{Control})\times100\%$, where $OD_{Control}$ and $OD_{Treated}$ were obtained in the absence and presence of CD_{Ara}, respectively.

2.6. Cellular imaging

A193 cells were cultured in DMEM supplemented with 10% FBS

and incubated at 37°C in a 5% CO_2 atmosphere. The CD_{Ara} aqueous solution (140 μL, 1.6 mg/mL) was added to the culture medium (1.0 mL) at 0.6 mg/mL final concentration. After incubation for 0.5 h, the A193 cells were harvested using 0.25% trypsin/0.020% EDTA, washed three times (1.0 mL each) with pH 7.4 phosphate buffered saline (PBS comprising137 mM NaCl, 2.7 mM KCl, 8.0 mM Na_2HPO_4, and 2.0 mM KH_2PO_4) and kept in PBS for optical imaging by a Olympus FV1000 confocal microscope (Tokyo, Japan) with 40 × objective.

2.7. Ex vivo carp imaging

Ex vivo imaging was carried out with a multispectral fluorescent vivo molecular imaging system (S-0010A). The carp was put in the water mixed with the CD_{Ara} (1.6 mg/mL). After 1 h, the fish was thoroughly rinsed with distilled water and imaged on the in vivo imaging system. Spectral fluorescence images were obtained using the appropriate filters for CD_{Ara} (excitation: 470 nm; emission: 515 nm long-pass filter; acquisition settings: 500–750 nm in 10 nm steps). Exposure times were automatically calculated and the acquisition setting was 1500 ms.

2.8. Patterning from CD solution

CD_{Ara} solution (1.6 mg/mL) is encapsulated into the pen for drawing versatile fluorescent patterns at room temperature. We take photographs with a multispectral fluorescent vivo molecular imaging system (S-0010A). Fluorescence patterns are obtained using the appropriate filters for CD_{Ara} (excitation: 470 nm; emission: 515 nm long-pass filter; acquisition settings: 500–750 nm in 10 nm steps). Exposure times were automatically calculated and the acquisition setting was 1500 ms.

2.9. Staining from CD solution

The filter papers are stained by CD_{Ara} solution (1.6 mg/mL) at room temperature. We take photographs with a multispectral fluorescent vivo molecular imaging system (S-0010A). Fluorescence photographs are obtained using the appropriate filters for CD_{Ara} (excitation: 470 nm; emission: 515 nm long-pass filter; acquisition settings: 500–750 nm in 10 nm steps). Exposure times were automatically calculated and the acquisition setting was 1500 ms.

3. Results and discussion

3.1. The synthesis of CDs

The successful fabrication of green fluorescent CDs is carried out by using petals as the starting materials via one-step hydrothermal method (Fig. 1). Petals contain sugar, protein, and ascorbic acid, which are widespread, easily available, low-cost, and green. Sugar and protein belong to carbohydrates and act as carbon precursors. At first hydrolysis, dehydration and decomposition of carbohydrates takes place in the presence of ascorbic acid and results in soluble compounds like furfural aldehydes, ketones and several organic acids like acetic, levulinic, formic acid, etc. Polymerization and condensation of these products transforms them into different soluble polymeric products. The aromatization and carbonization then take place via condensation and cycloaddition reactions. Finally CDs are obtained by a probable nuclear burst of these aromatic clusters at a critical concentration at the supersaturation point.[33] We discuss CDs derived from different precursors, such as Aralia petals, Hollyhock petals, Morning Glory petals, Lily petals, Chinese Rose petals, Sophora japonica petals, Azalea petals, Magnolia petals, and the yellow Rosa petals. The preparation of these CDs has been conducted in triplicate and the results are almost the same, which indicats good reproducibility of the product. As-prepared CDs freely disperse in water with transparent appearance. The pH value of these fresh CDs is ca. 5 because of the formation of carboxyl groups.

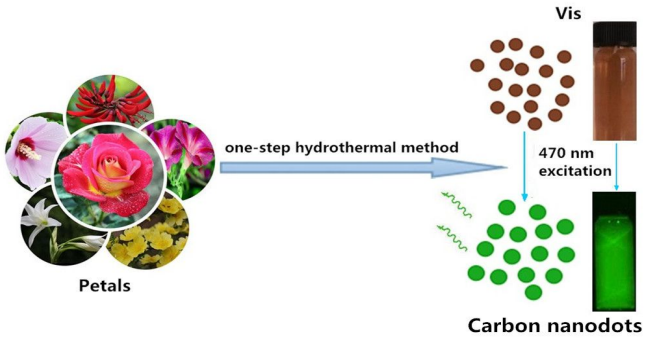

Fig. 1 Diagram for the synthesis of CDs from hydrothermal treatment of petals, along with photographs of the corresponding samples under daylight and 470 nm excitation.

3.2. The characterization of CDs

The optical properties of the CDs are displayed in Fig. 2 and 3. As shown in Fig. 2, the UV-vis absorption spectra of CD_{Ara}, CD_{Hol}, CD_{Mor}, CD_{Lil}, CD_{Ros}, CD_{SJ}, CD_{Aza}, CD_{Mag}, and CD_{Yel}, show similar broad absorptions from 220 to 400 nm. When excited at 470 nm, their PL spectra show the emission peaks at 510 nm, thus leading to a strong green fluorescent emission (the inset in Fig. 2). The green PL might be attributed to the combining effect of the emissive defects[34,35] and the decreased band gap[36] of CDs as a result of the higher graphitization degree.

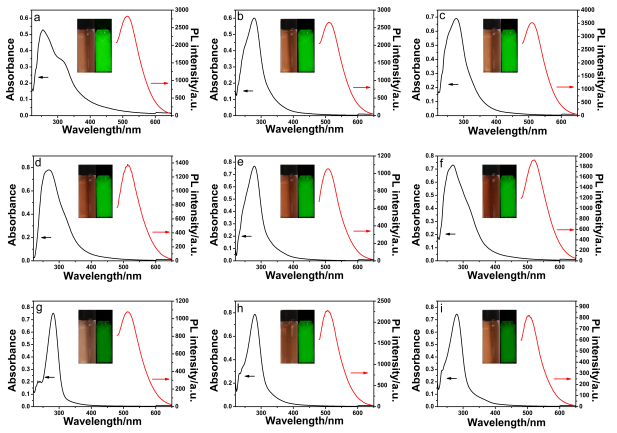

Fig. 2 Absorption and fluorescence emission spectra of (a) CD_{Ara}, (b) CD_{Hol}, (c) CD_{Mor}, (d) CD_{Lil}, (e) CD_{Ros}, (f) CD_{SJ}, (g) CD_{Aza}, (h) CD_{Mag}, and (i) CD_{Yel}. Inset: photographs of the corresponding samples under sunlight and 470 nm excitation.

To further explore the optical properties of CDs, the PL spectra of CDs under excitation wavelengths from 430 to 490 nm are measured (Fig. 3). With increasing excitation wavelength the PL intensity first increased and then decreased while the PL peak show red shift (the inset in Fig. 3), indicating that both PL

intensity and peak are dependent on excitation.

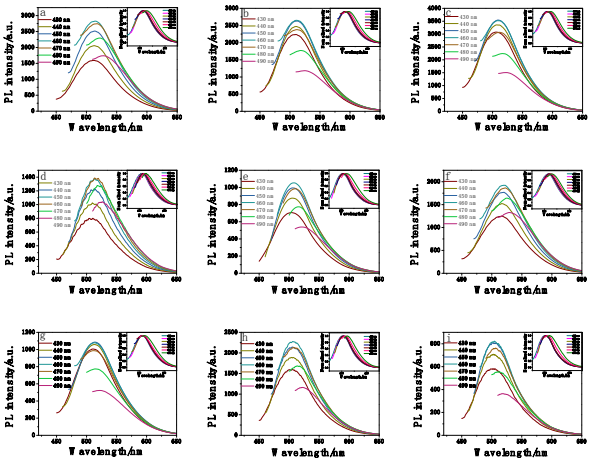

Fig. 3 Fluorescence spectra of (a) CD_{Ara}, (b) CD_{Hol}, (c) CD_{Mor}, (d) CD_{Lil}, (e) CD_{Ros}, (f) CD_{SJ}, (g) CD_{Aza}, (h) CD_{Mag}, and (i) CD_{Yel} at different excitation wavelengths. Inset: corresponding normalized spectra.

The fluorescence QY measured using Rhodamin 6G as a reference are 6.5%, 5.5%, 5.5%, 5.4%, 3.9%, 4.1%, 1.2%, 3.6%, and 1.9%, corresponding to CD_{Ara}, CD_{Hol}, CD_{Mor}, CD_{Lil}, CD_{Ros}, CD_{SJ}, CD_{Aza}, CD_{Mag}, and CD_{Yel}, respectively.

The composition of each kind of petals varies so the PL properties of as-prepared CDs are also different. To get good PL properties, we investigate the influence of different hydrothermal temperature and time on PL properties of the resultant CDs. Particularly, CD_{Ara}, CD_{Hol}, and CD_{Mor} were mainly discussed. In our experiments, hydrothermal temperature is selected as 200°C, 250°C, and 300°C and hydrothermal time is chosen as 2 h, 3 h, and 4 h. As shown in Fig. S1a–c, it seems that the optimum hydrothermal time is 3 h for syntheses of CD_{Hol} and CD_{Mor}, and 4 h for CD_{Ara}, respectively. As shown in Fig. S1d–f, it seems that the optimum hydrothermal temperature is 300°C for synthese of CD_{Ara}, CD_{Hol}, and CD_{Mor}.

The stability of the as-prepared CDs under different conditions is investigated. The PL intensity of CDs under pH from 3 to 10 is measured (Fig. 4a-c). It is very interesting to see that the PL intensity of CDs shifts slightly. In addition, we also study the influence of various external cations on the PL intensity of CDs. As shown in Fig. 4d-f, the PL intensity of CDs remains constant even the concentration of cations reaches up to 300 μM except that Cu^{2+} decrease the PL intensity a little. Additionally, the CDs have excellent stability that their PL intensity do not change even after continuous excitation for three hours (Fig. 4g-i) and storage for three months (Fig. 4j-l). This excellent tolerance to pH, external cations, and continuous excitation makes as-prepared CDs great potential in practical applications.

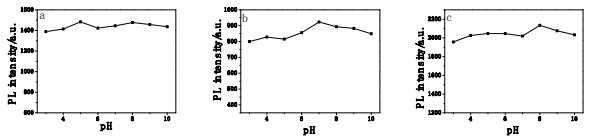

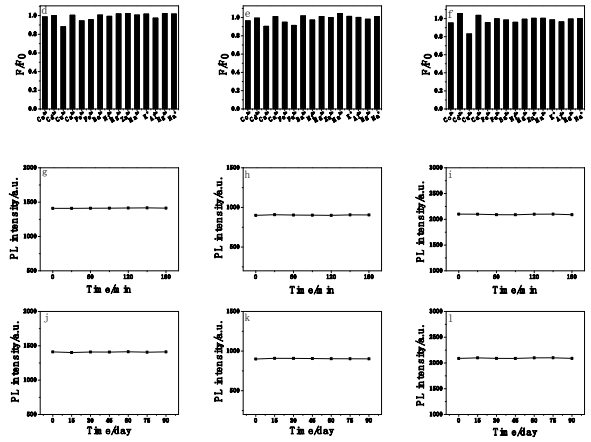

Fig. 4 Effect of pH on fluorescence intensity of (a) CD_{Ara}, (b) CD_{Hol}, and (c) CD_{Mor}. Effect of various external cations (300 μM) on fluorescence intensity of (d) CD_{Ara}, (e) CD_{Hol}, and (f) CD_{Mor}. Dependence of fluorescence intensity on excitation time of (g) CD_{Ara}, (h) CD_{Hol}, and (i) CD_{Mor}. Dependence of fluorescence intensity on storage time of (j) CD_{Ara}, (k) CD_{Hol}, and (l) CD_{Mor}.

Fluorescence lifetime is the characteristic period that the CDs remain in its excited state prior to returning to its ground state. Typically measured in nanoseconds, fluorescent lifetime is an intrinsic property of CDs depending on the nature of the fluorescent sites and the environment. The fluorescence lifetime (τ) of CDs is assessed by fluorescent decay curves. As seen in Fig. S2a-c, the fluorescent decay curves of the CD solution are recorded at 510 nm under 470 nm excitation. The decay curves are fitted using exponential functions $Y(t)$ based on a non-linear least squares analysis using the following equation: $Y(t) = A_1\exp(-t_1/\tau_1) + A_2\exp(-t_2/\tau_2)$, where A_1 and A_2 are the fractional contributions of time-resolved decay lifetime of τ_1 and τ_2. We calculated the average lifetime of CD_{Ara} , CD_{Hol}, and CD_{Mor} to be 6.0868 ns , 5.7917 ns, and 5.8015 ns, respectively.

The surface functional groups of CDs are characterized by FTIR. In FTIR spectra of CDs (Fig. 5a), the peaks at 3401 and 2952 cm^{-1} are attributed to the O−H and CH_2 stretching vibrations, the peaks at about 1603 cm^{-1} and 1088 cm^{-1} are attributed to the C=O and C−O stretching vibrations, and the peak at 1384 cm^{-1} is ascribed to the CH_2 bending vibrations. The FTIR results confirm that the synthesized CDs are functioned with carboxylic moieties. We also used XPS to identify the functional groups and element states of CDs. The XPS analysis of the elemental composition of CDs demonstrates that these CDs are mainly composed of C and O element (the atom ratio of C:O is 1.91:1). The XPS spectrum of the CDs (Fig. 5b) shows two peaks at 290.0 and 530.0 eV. The first corresponds to C_{1s} and another one corresponds to O_{1s}. The C_{1s} spectrum of the CDs indicates the presence of four types of carbon bonds: C=C (284.8 eV), C−C (286.2 eV), C=O (287.6 eV) and O=C−O (288.6 eV) (Fig. 5c). In the O_{1s} spectrum (Fig. 5d), the peaks at 532.0 and 532.8 eV are ascribed to C=O and C−OH/C−O−C. The functional groups identified by the XPS are in good agreement with FTIR. The zeta potential of CDs is −19.1 mV, due to the existence of −OH/−COOH groups on the surface of CDs. The surface of prepared CDs is covered with carboxyl groups and negatively charged. Because the same charges repel each other, CDs do not

aggregate.

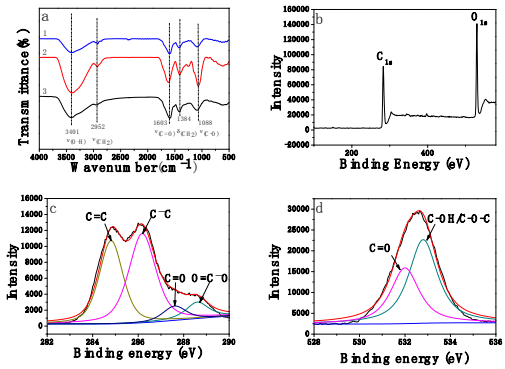

Fig. 5 (a) FTIR spectra of CDs (1. CD_{Ara}, 2. CD_{Hol}, and 3. CD_{Mor}). (b) XPS survey spectrum of CD_{Ara}. (c) C_{1s} spectrum of CD_{Ara}. (d) O_{1s} spectrum of CD_{Ara}.

The size distribution and morphology of CD_{Ara} are characterized by TEM (Fig. 6). As shown in Fig. 6a-b, CDs are spherical in morphology and well dispersed. The histogram in Fig. 6c demonstrates that the size distribution of the CDs is relatively small and the majority falls within the range from 1.5 to 4.0 nm. Based on the statistical analysis of above 132 particles, the average diameter of the CDs is 2.49 ± 0.13 nm. The high resolution TEM (HRTEM) images (Fig. 6d-e) show a crystalline structure with lattice spacing of 0.205 nm which may be attributable to the (102) facet of graphite.[15] The SAED of CDs (Fig. 6f) indicates the CDs is monocrystal.

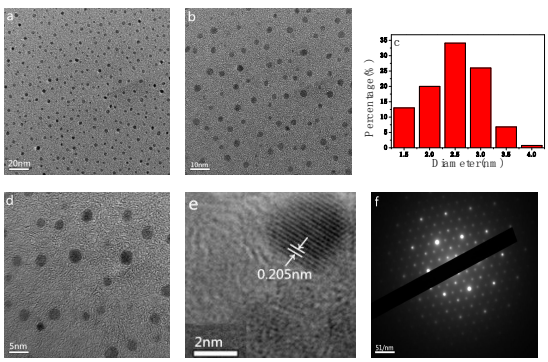

Fig. 6 TEM images of CD_{Ara} (a) scale bar is 20 nm and (b) scale bar is 10 nm. (c) Diameter distributionof CD_{Ara}. HRTEM images of CD_{Ara} (d) scale bar is 5 nm, and (e) scale bar is 2 nm. (f) SAED of CD_{Ara}.

3.3. Cell cytotoxicity assay

To explore the potential application of CDs in living cell imaging, the cytotoxicity of CD_{Ara} is evaluated by the MTT assay in A193 cells. In the MTT assay, MTT could be reduced by the active cellular enzymes in the cells to insoluble blue-violet formazan crystals. The quantitative information about the cytotoxicity of CD_{Ara} would be obtained by the measurement of absorption on the cells. We perform the MTT assay in A193 cells with concentrations from 0.1 mg/mL to 0.8 mg/mL. The results demonstrate that more than 85% of cells are viable (Fig. S3), showing the low toxicity of CD_{Ara} to cultured cells under the experimental conditions at the concentration of 0.6 mg/mL.

3.4. Living cell imaging of CDs

To assess the potential application of CDs as a bioimaging probe, A193 cells are cultured in the medium containing 0.6 mg/mL CD_{Ara} for 0.5 h at 37°C, and then observed under confocal microscope. Bright-field image after CD_{Ara} incubation confirms the viability of the cells (Fig. 7a and d). Under 488 nm excitation, CD_{Ara} with green fluorescence emission disperse well within living cells, indicating excellent cell membrane permeability (Fig. 7b and e). According to the clear cell morphology (Fig. 7a, c, d, and f), the PL spots are observed not only in the cytoplasmic area of the cell but also in the nucleus of the cell, indicating that the CD_{Ara} easily penetrate into the whole cell. Moreover, analyses of confocal microscopy also indicate that the photo stability of CD_{Ara} is remarkably high, with no blinking and low photobleaching.

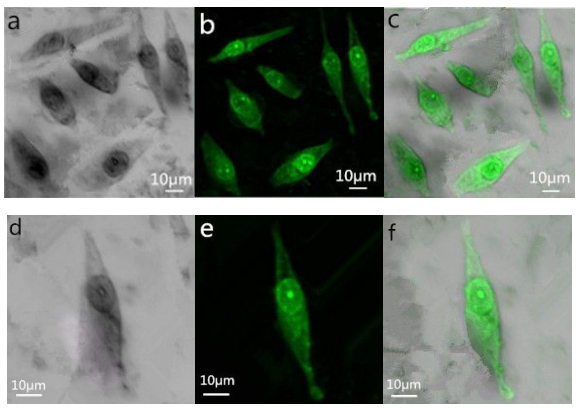

Fig. 7 Confocal fluorescence images of A193 cells incubated with 0.6 mg/mL CD_{Ara} for 0.5 h under (a) bright-field and (b) 488 nm excitation. (c) The merged image of a and b. Confocal fluorescence images of selected A193 cell incubated with 0.6 mg/mL CD_{Ara} for 0.5 h under (d) bright-field and (e) 488 nm excitation. (f) The merged image of d and e.

3.5. Ex vivo carp imaging of CDs

For organisms imaging, carps are selected because they are small aquatic craniate animals. As shown in Fig. 8b, the CD_{Ara} labelled carp (center) clearly showes enhanced luminescence as compared with its control (left) with a signal-to-noise ratio of 2.88. Fluorescence spectra analysis confirms that the fluorescence signal is coming from the CD_{Ara}. This result suggests that the CD_{Ara} might have potential for small aquatic craniate animals imaging.

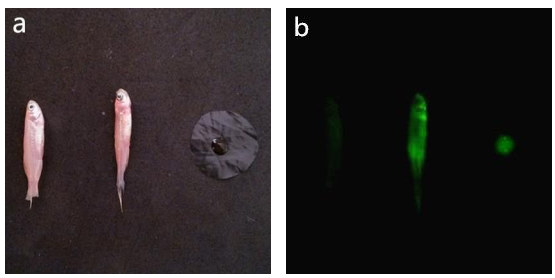

Fig. 8 CD_{Ara} for ex vivo carp imaging under (a) sunlight and (b) 470 nm excitation.

3.6. CDs for patterning

We apply the CD_{Ara} as fluorescent ink for producing various patterns, which shows clear green fluorescence (Fig. 9). Notably, these patterns drawn from CD_{Ara} solution are invisible under daylight but visible under 470 nm excitation. The "vis-invisible" properties of CD_{Ara} benefit their applications in anti-counterfeit fields as well as optoelectronic devices.[17]

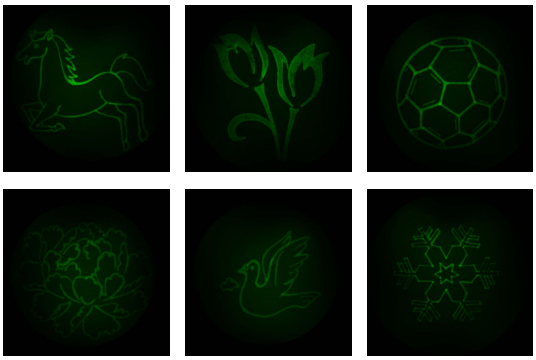

Fig. 9 Different photographs of the fluorescent patterns under 470 nm excitation.

3.7. CDs for staining

The CD_{Ara}, serving as fluorescent dye, are used for staining (Fig. 10). The filter papers with staining present dramatic fluorescence under 470 nm excitation. Hence, these photographs strongly demonstrate that the fluorescent CD_{Ara} could serve for staining.

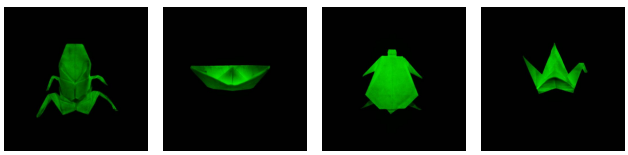

Fig. 10 Different images of filter papers stained by CD_{Ara} under 470 nm excitation.

4. Conclusions

We have described an easy, green, and economic route for fabricating green fluorescent CDs with the use of ubiquitous and natural plant petals as the precursor via one-step hydrothermal method. The as-prepared CDs show good fluorescence without further surface treatment. In addition, CDs display excellent stability towards various conditions, including pH, external metal cations, and continuous excitation. CDs can be taken up by cell and ex vivo fish, which suggests that the CDs may have potential applications in biolabelling and bioimaging. Moreover, we also apply the CDs as fluorescent ink and fluorescent dye, which may expand the potential applications of CDs in anti-counterfeit and optoelectronic applications.

Acknowledgements

This work was supported by the National Natural Science Foundation of China (21175086 and 21306108), Natural Science Foundation of Shanxi Province of China (2013011009-5 and 2014011016-2), and Shanxi Scholarship Council of China (No.2014-018), Innovative Talents in Higher School Support Plan (2014107), Hundred Talent Program of Shanxi Province, and Technology Foundation for Selected Overseas Chinese Scholar in Shanxi Province.

Notes and references

[a]*College of Chemistry and Chemical Engineering, Institute of Environmental Science, Shanxi University, Taiyuan 030006, PR China*
[b]*Taiyuan University, Taiyuan 030012, PR China*
* *Corresponding author: Fax: +86-531-7018842; Tel: +86-531-7011688;*
E-mail addresses: shilihong@sxu.edu.cn (Lihong Shi).

1 L. H. Shi, X. F. Li, Y. Y. Li, X. P. Wen, J. F. Li, M. F. C. Martin, C. Dong and S. M. Shuang, *Sen. Act. B*, 2015, **210**, 533.
2 S. N. Baker and G. A. Baker, *Angew. Chem. Int. Ed.*, 2010, **49**, 6726.
3 J. Y. Hou, J. Dong, H. S. Zhu, X. Teng, S. Y. Ai and M. L. Mang, *Biosens. Bioelectron.*, 2015, **68**, 20.
4 L. Zhou, Y. Lin, Z. Huang, J. Ren and X. Qu, *Chem. Commun.*, 2012, **48**, 1147.
5 Z. L. Wu, M. X. Gao, T. T. Wang, X. Y. Wan, L. L. Zheng, and C. Z. Huang, *Nanoscale,* 2014, **6**, 3868.
6 B. X. Zhang, G. Y. Zhang, H. Gao, S. H. Wu, J. H. Chen and X. L. Li, *RSC. Adv.*, 2015, **5**, 7395.
7 C. J. Liu, P. Zhang, X. Y. Zhai, F. Tian, W. C. Li, J. H. Yang, Y. Liu, H. B. Wang, W. Wang and W. G. Liu, *Biomaterials*, 2012, **33**, 3604.
8 Y. L. Jiang, Q. R. Han, C. Jin, J. Zhang and B. X. Wang, *Mater. Lett.*, 2015, **5**, 7395.
9 H. T. Li, X. D. He, Z. H. Kang, H. Huang, Y. Liu, J. L. Liu, S. Y. Lian, C. H. A. Tsang, X. B. Yang and S. T. Lee, *Angew. Chem. Int. Ed.*, 2010, **49**, 4430.
10 D. M. Wang, M. X. Gao, P. F. Gao, H. Yang and C. Z. Huang, *J. Phys. Chem. C*, 2013, **117**, 19219.
11 S. N. Qu, X. Y. Wang, Q. P. Lu, X. Y. Liu and L. J. Wang, *Angew. Chem. Int. Ed.*, 2012, **51**, 12215.
12 W. B. Shi, Q. L. Wang, Y. J. Long, Z. L. Cheng, S. H Chen, H. Z. Zheng and Y. M. Huang, *Chem. Commun.*, 2011, **47**, 6695.
13 S. L. Hu, K. Y. Niu, J. Sun, J. Yang, N. Q. Zhao and X. W. Du, *J. Mater. Chem.*, 2009, **19**, 484.
14 Q. L. Zhao, Z. L. Zhang, B. H. Huang, J. Peng, M. Zhang and D. W. Pang, *Chem. Commun.*, 2008, 5116.
15 J. G. Zhou, C. Booker, R. Y. Li, X. T. Zhou, T. K. Sham, X. L. Sun and Z. F. Ding, *J. Am. Chem. Soc.*, 2007, **129**, 744.
16 Z. A. Qiao, Y. F. Wang, Y. Gao, H. W. Li, T. Y. Dai, Y. L. Liu, and Q. S. Huo, *Chem. Commun.*, 2010, **46**, 8812.
17 L. L. Zhu, Y. J. Yin, C. F. Wang and S. Chen, *J. Mater. Chem. C*, 2013, **1**, 4925.
18 C. W. Lai, Y. H. Hsiao, Y. K. Peng and P. T. Chou, *J. Mater. Chem.*, 2012, **22**, 14403.
19 D. Sun, R. Ban, P. H. Zhang, G. H. Wu, J. R. Zhang and J. J. Zhu, *Carbon*, 2013, **64**, 424.
20 H. Y. Ko, Y. W. Chang, G. Paramasivam, M. S. Jeong, S. Cho and S. Kim, *Chem. Commun.*, 2013, **49**, 10290.
21 Z. L. Wu, P. Zhang, M. X. Gao, C. F. Liu, W. Wang, F .Lenga and C. Z. Huang, *J. Mater. Chem. B*, 2013, **1**, 2868.
22 C. Z. Zhu, J. F. Zhai and S. J. Dong, *Chem. Commun.*, 2012, 48, 9367.
23 Y. H. Yang, J. H. Cui, M. T. Zheng, C. F. Hu, S. Z. Tan, Y. Xiao, Y. Qu and Y. L. Liu, *Chem. Commun.*, 2012, **48**, 380.
24 Z. C. Yang, M. Wang, A. M. Yong, S. Y. Wong, X. H. Zhang, H. Tan, A. Y. Chang, X. Li and J. Wang, *Chem. Commun.*, 2011, **47**, 11615.
25 J. Jiang, Y. He, S. Y. Li and H. Cui, *Chem. Commun.*, 2012, **48**, 9634.
26 A. Prasannan and T. Imae, *Ind. Eng. Chem. Res.*, 2013, **52**, 15673.
27 J. M. Wei, X. Zhang, Y. Z. Sheng, J. M. Shen, P. Huang, S. K. Guo, J. Q. Pan, B. T. Liu and B. X. Feng, *New J. Chem.*, 2014, **38**, 906.
28 Y. P. Sun, X. Wang, F. S. Lu, L. Cao, M. J. Meziani, P. G. Luo, L. R. Gu and L. M. Veca, *J. Phys. Chem. C*, 2008, **112**, 18295.
29 Y. Liu, C. Y. Liu and Z. Y. Zhang, *J. Mater. Chem. C*, 2013, **1**, 4902.
30 W. Wang, Y. M. Li, L. Cheng, Z. Q. Cao and W. G. Liu, *J. Mater. Chem. B*, 2014, **2**, 46.
31 Y. Liu, N. Xiao, N. Q. Gong, H. Wang, X. Shi, W. Gu and L. Ye, *Carbon*, 2014, **68**, 258.

32 Y. S. Li, X. X. Zhong, A. E. Rider, S. A. Furmand and K. Ostrikov, *Green Chem.*, 2014, **16**, 2566.
33 B. De and N. Karak, *RSC Adv.*, 2013, **3**, 8286.
34 Y. P. Sun, B. Zhou, Y. Lin, W. Wang, K. A. S. Fernando, P. Pathak, M. J. Meziani, B. A. Harruff, X. Wang, H. F. Wang, P. G. Luo, H. Yang, M. E. Kose, B. L. Chen, L. M. Veca and S.Y. Xie, *J. Am. Chem. Soc.* 2006, **128**, 7756.
35 S. J. Zhu, J. H. Zhang, S. J. Tang, C. Y. Qiao, L. Wang, H. Y. Wang, X. Liu , B. Li , Y. F. Li , W. L. Yu , X. F. Wang , H. C. Sun and B. Yang, *Adv. Funct. Mater.*, 2012, **22**, 4732.
36 Y. X. Fang, S. J. Guo, D. Li, C. Z. Zhu, W. Ren, S. J. Dong and E. K. Wang, *ACS. Nano.*, 2012, **6**, 400.